HHS Public Access

Author manuscript

Mol Neurobiol. Author manuscript; available in PMC 2020 October 01.

Published in final edited form as:

Mol Neurobiol. 2019 October ; 56(10): 7085–7096. doi:10.1007/s12035-019-1545-y.

Fn14 participates in neuropathic pain through NF-κB pathway in primary sensory neurons

Li-Na Huang[1,2,*], **Yun Zou**[1,2,*], **Shao-Gen Wu**[1], **Hong-Hong Zhang**[1], **Qing-Xiang Mao**[1], **Jin-Bao Li**[2], **Yuan-Xiang Tao**[1]

[1]Department of Anesthesiology, New Jersey Medical School, Rutgers, The State University of New Jersey, Newark, NJ 07103, USA

[2]Department of Anesthesiology, Shanghai General Hospital, Shanghai Jiao Tong University School of Medicine, (Original named “Shanghai First People’s Hospital”), Shanghai 200080, China

Abstract

Fibroblast growth factor-inducible-14 (Fn14), a receptor for tumor necrosis-like weak inducer of apoptosis, is expressed in the neurons of dorsal root ganglion (DRG). Its mRNA is increased in the injured DRG following peripheral nerve injury. Whether this increase contributes to neuropathic pain is unknown. We reported here that peripheral nerve injury caused by spinal nerve ligation (SNL) increased the expression of Fn14 at both protein and mRNA levels in the injured DRG. Blocking this increase attenuated the development of SNL-induced mechanical, thermal, and cold pain hypersensitivities. Conversely, mimicking this increase produced the increases in the levels of phosphorylated extracellular signal-regulated kinase ½ and glial fibrillary acidic protein in ipsilateral dorsal horn and the enhanced responses to mechanical, thermal, and cold stimuli in the absence of SNL. Mechanistically, the increased Fn14 activated the NF-κB pathway through promoting the translocation of p65 into nucleus of the injured DRG neurons. Our findings suggest that Fn14 may be a potential target for the therapeutic treatment of peripheral neuropathic pain.

Keywords

Fn14; NF-κB pathway; primary sensory neurons; neuropathic pain

Corresponding authors: Dr. Yuan-Xiang Tao, Department of Anesthesiology, New Jersey Medical School, Rutgers, The State University of New Jersey, 185 S. Orange Ave., MSB, E-661, Newark, NJ 07103. Tel: +1-973-972-9812; Fax: +1-973-972-1644. yuanxiang.tao@njms.rutgers.edu or. Dr. Jinbao Li, Department of Anesthesiology, Shanghai General Hospital, Shanghai Jiao Tong University School of Medicine, No 86, Wujin Road, Hongkou District, Shanghai 200080, China. Tel:+1-862163240090-7402; lijinbaoshanghai@163.com.

*LH and YZ equally contributed to this work.

Compliance with Ethical Standards

The Institutional Animal Care and Use Committee at New Jersey Medical School, Rutgers approved all experimental procedures (IACUC approved number 13035A2E0716).

Conflicts of interests

The authors declare no competing interests.

Introduction

Nerve injury-induced neuropathic pain is a complex and debilitating public health concern that affects the quality of life of approximately seven percent of the world population [1–3]. Over 100 billion dollars are spent each year on chronic pain-related healthcare expenses and lost productivities. Current successful treatment options for this disorder are limited [4,5]. Although opioids are still the gold standards for pharmacological treatment of neuropathic pain, they cause severe adverse effects [6–8]. Particularly, the increase in opioid prescriptions recently in the United States has been accompanied by a huge increase in the incidence of addiction and opioid-related mortality [9] . Thus, identifying novel mechanisms of neuropathic pain is essential for the discovery of new treatments and preventive tactics for this disorder.

The transmembrane protein fibroblast growth factor-inducible-14 (Fn14) is a receptor for tumor necrosis-like weak inducer of apoptosis (TWEAK), a member of the tumor necrosis factor superfamily of structurally related cytokines [10]. TWEAK binding to Fn14 promotes cell proliferation, migration, and differentiation, as well as the expression of proinflammatory molecules [11]. Fn14 has been demonstrated to be associated with autoimmune diseases, lung injury, impaired renal function, abnormal endothelial cell proliferation, and skeletal muscle atrophy [12–18]. In the central nervous system, TWEAK targets endothelial cells, astrocytes, and neurons [19–21]. The TWEAK-Fn14 signaling pathway participates in neurodegenerative diseases, multiple sclerosis, neuropsychiatric systemic lupus erythematosus, stroke, and glioma [12,22–24]. Although a previous study showed a TWEAK-independent increase in the expression of Fn14 in neurons of dorsal root ganglion (DRG) during sciatic nerve regeneration [18], the role of DRG Fn14 in nerve injury-induced neuropathic pain is unknown.

In this study, we first observed whether peripheral nerve injury increased the expression of Fn14 in the DRG in the preclinical mouse model of unilateral fourth lumbar spinal nerve ligation (SNL)-induced neuropathic pain. We then examined whether this increase contributed to the development and maintenance of SNL-induced pain hypersensitivities. We finally elucidated how this increase participated in nerve injury-induced neuropathic pain.

Materials and Methods

Animal preparations

The experimental procedures were approved by the Animal Care and Use Committee at New Jersey Medical School and all the experiments were performed in accordance with the ethical guidelines of the US National Institutes of Health and the International Association for the Study of Pain. The CD1 male mice (7–8 weeks) were purchased from Charles River Laboratories (Wilmington, MA). To minimize intra- and inter-individual variability of behavioral outcome measures, mice were trained for 1–2 days before behavioral testing was carried out. All efforts were made to minimize animal suffering and reduce the number of animals used. The experimenters were blinded to treatment condition during behavioral testing.

Neuropathic pain models

SNL-induced neuropathic pain model in mice was carried out as described previously [25]. Briefly, the CD1 mice were anesthetized with 2–3% isoflurane. The left fourth lumbar (L4) transverse process was identified and then removed. The underlying L4 spinal nerve was carefully isolated and tightly ligated with a 7–0 silk suture under a surgical microscope. The ligated nerve was then transected just distal to the ligature. The skin and muscles were closed in layers. The surgical procedure for the sham surgical group was identical to that for the SNL group, except that the spinal nerve was not transected and ligated.

The CCI-induced neuropathic pain model was carried out with minor modification, as described previously [26]. Briefly, mice were placed under anesthesia with isoflurane. The sciatic nerve was exposed and loosely ligated with 7–0 silk thread at three sites with an interval of about 1mm proximal to trifurcation of the sciatic nerve. Sham animals received an identical surgery but without the ligation.

Behavioral tests

Mechanical test was carried out as described previously [27,26,28]. Briefly, the mice were placed individually in a Plexiglas chamber on an elevated mesh screen and allowed to habituate for 30 min. The calibrated von Frey filament (0.4 g, Stoelting Co.) was used to stimulate the hind paw for 1–2 s and repeated 10 times on both hind paws with 5min interval. A quick withdrawal of the paw was regarded as a positive response. Paw withdrawal frequency was calculated as follow: (number of paw withdrawals/10 trials) × 100%.

Heat test was performed as described [28,27,26]. Briefly, paw withdrawal latency to noxious heat was measured with a Model 336 Analgesia Meter (IITC Inc. Life Science Instruments. Woodland Hills, CA). The mice were placed in a Plexiglas chamber on a glass plate. A beam of light was emitted from the light box and applied on the middle of the plantar surface of each hind paw. A quick lift of the hind paw was regarded as the signal to turn off the light. The length of lighting beam time was defined as the paw withdrawal latency. For each side, five trials with 5-min interval time were carried out. A cutoff time of 20 s was used to avoid tissue damage.

Cold test was carried out by measuring paw withdrawal latencies to noxious cold (0 °C) using a cold aluminum plate as described [28,27,26]. Briefly, each mouse was placed in a Plexiglas chamber on the plate with continuous temperature monitoring by a thermometer. The length of time between the placement and the sign of mouse jumping was defined as the paw jumping latency. Each trial was repeated three times at 10-min intervals. A cutoff time of 20 s was used to avoid tissue damage.

Conditional place preference test was carried out as described [29]. Briefly, an apparatus with two Plexiglas chambers connected with an internal door (Med Associates Inc.) was used. One of the chambers was made of rough floor and walls with black and white horizontal stripes and another one was composed of a smooth floor and walls with black and white vertical stripes. Movement of the mice and time spent in each chamber were monitored by photobeam detectors installed along the chamber walls and automatically

recorded in MED-PC IV CPP software. Mice were first preconditioned for 30 min with full access to two chambers to habituate them to the environment. At the end of the preconditioning phase, the basal duration time spent in each chamber was recorded within 15 min to check whether mice had a preexisting chamber bias. Animals spending more than 80% or less than 20% of the total time in any chamber were excluded from further testing. The conditioning protocol was performed for the following 3 days with the internal door closed. The mice first received intrathecal injection of saline (5 μl) specifically paired with one conditioning chamber in the morning. Six hours later, lidocaine (0.8 % in 5 μl of saline) was given intrathecally paired with another conditioning chamber in the afternoon. Injection order of saline and lidocaine every day was switched. On the test day, at least 20 hours after the conditioning, the mice were placed in one chamber with free access to both chambers. The duration of time that each mouse spent in each chamber was recorded for 15 min. Difference scores were calculated through subtracting preconditioning time by test time spent in the lidocaine chamber.

Locomotor functional tests, including placing, grasping, and righting reflexes, were carried out after the pain behavioral tests described above were completed [30]. For the placing reflex, the hind limbs were placed slightly lower than the forelimbs and the dorsal surfaces of the hind paws were brought into contact with the edge of a table. Then, data on whether or not the hind paws were placed on the table surface reflexively was recorded. For the grasping reflex, animals were placed on a wire grid, and data on whether or not the hind paws grasped the wire on was recorded. For the righting reflex, animals were placed on its back on a flat surface, and data was recorded on whether or not the mouse could immediately assume the normal upright position. Each trial was repeated five times with 5-min intervals in between and the score for each test was determined by counting the number of times a normal reflex was observed.

DRG microinjection

DRG microinjection was carried out as described previously [27,26]. For knockdown experiments, the adeno-associated virus serotype 5 (AAV5) was microinjected into ipsilateral L4 DRG 35 days before SNL/sham surgery. For overexpression experiments, AAV5 was microinjected into unilateral L3/4 DRGs of naive mice. Briefly, a dorsal midline incision was made in the lower lumbar region. The left L3/4 articular processes were exposed and then removed. After the DRG was exposed, AAV5 viral solution (1 μl/DRG, 2× 1013 tu/μl) was injected into the DRG with a glass micropipette connected to a Hamilton syringe. The pipette was removed 10 min after injection. The surgical field was irrigated with sterile saline and the skin incision was closed with wound clips.

Western blot analysis

Two unilateral DRGs from two mice were pooled together to achieve enough proteins. The tissues were homogenized and the cultured cells ultrasonicated in chilled lysis buffer (10 mM Tris, 1 mM phenylmethylsulfonyl fluoride, 5 mM $MgCl_2$, 5 mM EGTA, 1 mM EDTA, 1mM DTT, 40 μM leupeptin, 250 mM sucrose). Approximately 10% of the homogenates in volume were used for total proteins. The remaining was centrifuged at 4 °C for 15 min at 1,000 g. The supernatant was collected for cytosolic proteins and the pellet for nuclear

proteins. After the concentrations of the proteins in the samples were measured using the Bio-Rad protein assay (Bio-Rad), the samples were heated at 99 °C for 5 min and loaded onto a 4–15% stacking/7.5% separating SDS-polyacrylamide gel (Bio-Rad). The proteins were then electrophoretically transferred onto a polyvinylidene difluoride membrane (Bio-Rad). The membrane was first blocked with 3% nonfat milk in Tris-buffered saline containing 0.1% Tween-20 for 1 h at room temperature and then incubated at 4oC overnight with the following primary antibodies: rabbit anti-Fn14 (1:1,000; CST), rabbit anti-p65 (1:1,000; CST), rabbit anti-GAPDH (1:1,000; Santa Cruz), rabbit anti-H3 (1:1,000; Santa Cruz) , mouse anti-glial fibrillary acidic protein (GFAP; 1:1,000; Abcam), rabbit anti-phosphorylated extracellular signal-regulated kinase ½ (p-ERK1/2; 1:1,000; CST), rabbit anti-total extracellular signal-regulated kinase ½ (ERK1/2; 1:1000; CST). The proteins were detected by horseradish peroxidase–conjugated anti-mouse or anti-rabbit secondary antibody (1:3,000; Jackson ImmunoResearch) and visualized by western peroxide reagent and luminol/enhancer reagent (Clarity Western ECL Substrate, Bio-Rad). Exposure was done using ChemiDoc XRS and System with Image Lab software (Bio-Rad). The intensity of blots was quantified with densitometry using Image Lab software (Bio-Rad). All cytosol protein bands were normalized to GAPDH, whereas all nucleus protein were normalized to total histone H3.

Quantitative real-time RT-PCR

Total RNA extraction and quantitative real-time RT-PCR were carried out as described [26,27,31]. Briefly, unilateral L4 DRGs from four adult mice were collected rapidly and pooled together to achieve enough RNA. Total RNA was extracted by miRNeasy kit (Qiagen, Valencia, CA) according to manufacturer's instructions, and reverse-transcribed using the ThermoScript Reverse Transcriptase (Invitrogen/Thermo Fisher Scientific) with oligo (dT) primers (Invitrogen/Thermo Fisher Scientific). Template (1 μl) was amplified in a Bio-Rad CFX96 real-time PCR system using specific primers listed on Supplementary Table 1. Each sample was run in triplicate in a 20μl reaction volume containing 250 nM forward and reverse primers, 10 μl of SsoAdvanced Universal SYBR Green Supermix (Bio-Rad Laboratories), and 20 ng of cDNA. The PCR amplification consisted of 30 s at 95°C, 30 s at 60°C, 30 s at 72°C, and 5 min at 72°C for 39 cycles. Ratios of ipsilateral-side mRNA levels to contralateral-side mRNA levels were calculated using the ΔCt method ($2^{-\Delta\Delta Ct}$) after normalization to *Tuba-1a* as it has been demonstrated to be stable even after peripheral nerve injury insult in mice as shown previously[31].

Single cell real-time RT-PCR

Single cell real-time RT-PCR was carried out as described previously[27,26]. Briefly, freshly cultured DRG neurons from mice were prepared as described before[31,32]. Four hours after plating, a single living DRG neuron (large: > 35 μm; medium: 25–35 μm; small: < 25 μm) was collected in a PCR tube with 10 μl of cell lysis buffer (Signosis, Sunnyvale, CA) under an inverted microscope fit with a micromanipulator and microinjector. After centrifugation, the supernatants were harvested and divided into three PCR tubes, respectively, for *Tnfrsf12a* (encoding Fn14 protein), *Rela* (encoding p65 protein) and *Gapdh* (as a positive control) mRNAs. The primers used are listed in Supplementary Table 1. The remaining real-

time RT-PCR procedures were carried out based on the manufacturer's protocol with the single-cell real-time RT-PCR assay kit (Signosis).

Plasmid construction and virus production

A *Tnfrsf12a* shRNA duplex was designed corresponding to bases 583–601 of the mouse *Tnfrsf12a* mRNA (GenBank accession number NM_013749). The oligonucleotides harboring the shRNA sequences were synthesized and annealed. A mismatch shRNA with a scrambled sequence and no known homology to a mouse gene (scrambled shRNA) was used as a control. The fragments were ligated into the pro-viral plasmid by BamH1/XbaI restriction sites. To construct a plasmid that expresses Fn14 protein, the full-length sequences of *Tnfrsf12a* mRNA from mouse DRG was reverse-transcribed and amplified by PCR and primers (Supplementary Table 1). The resulting segment was digested by EcoRI and BamHI and then inserted into the pro-viral plasmid. The resulting vectors expressed the genes under the control of the cytomegalovirus promoter. The recombinant clones were verified by using DNA sequencing. The AAV5 viral particles were prepared using AAV5 Helper Free Packaging System (Cell Biolabs, Inc., San Diego, CA). The AAV5 particles were purified using AAVpro Purification Kit (Takara, Mountain View, CA).

Statistical analysis

Animals were assigned into various treatment groups randomly. All results are given as means ± S.E.M. One-way or two-way repeated analysis of variance (ANOVA) with the *post hoc* Tukey testing and paired or unpaired Student's t-test were applied for normally distributed data, and the Mann-Whitney U-test was used for non-parametric data (SigmaPlot 12.5, San Jose, CA). Significance was set at $P < 0.05$.

Results

Fn14 expression is increased in the ipsilateral DRG after SNL

We first examined the Fn14 expression in the DRG after SNL and sham surgery. Basal level of Fn14 protein expression was relatively lower in the DRG of sham or naive mice. SNL time-dependently increased the expression of *Tnfrsf12a* mRNA and its encoding Fn14 protein in the L4 DRG on the ipsilateral side, but not on the contralateral side (Fig. 1). The levels of *Tnfrsf12a* mRNA in the ipsilateral L4 DRG were increased by 7.4-fold on day 3, 5.9-fold on day 7, and 5.4-fold on day 14 after SNL compared to in sham surgery mice at the corresponding time points (Fig. 1A). The amounts of Fn14 protein in the ipsilateral L4 DRG were increased by 2.2-fold on day 3, 2.5-fold on day 7, and 3.3-fold on day 14 compared to the corresponding contralateral L4 DRG after SNL (Fig. 1B). As expected, sham surgery did not alter basal levels of Fn14 protein in the ipsilateral L4 DRG (Fig.1, C). Fn14 protein in the ipsilateral L3 DRG during the observation period did not change (Fig.1, D). SNL and sham surgery did not change basal amounts of *Tnfrsf12a* mRNA (data not shown). We also tested Fn14 protein expression in the ipsilateral L3/4 DRGs after CCI, another established neuropathic pain model. The level of Fn14 protein was increased by 2.2-fold on day 7 post-CCI compared to the corresponding sham surgery mice (Fig. 1E).

Intrathecal Fn14 inhibitor alleviates SNL-induced neuropathic pain

We then observed whether inhibition of DRG Fn14 affected SNL-induced pain hypersensitivity. On day 3 after SNL or sham surgery, the Fn14 inhibitor L524–0366 (dissolved in 5% DMSO; Focus Biomolecular LLC, Plymouth Meeting, PA) or vehicle (5% DMSO, dissolved in saline) with total volume of 5 μl was injected intrathecally. Behavioral tests were carried out one day prior to surgery, before injection, and 15, 30, 45, 60, 90 and 120 min after injection on day 3 post-surgery. Consistent with the previous studies [33,27], SNL, but not sham surgery, produced mechanical allodynia, thermal hyperalgesia, and cold allodynia on the ipsilateral side on day 3 post-SNL (Fig. 2). Compared with the sham plus vehicle group, paw withdrawal frequencies in response to mechanical stimulation were significantly increased and paw withdrawal latency in response to heat and cold stimuli markedly reduced in the SNL plus vehicle group (Fig. 2A-2C). These pain hypersensitivities were time-dependently attenuated on the ipsilateral side after intrathecal injection of L524–0366 at 20 μg in SNL mice (Fig. 2A-2C). The paw withdrawal frequencies in response to mechanical stimulation applied to the ipsilateral hindpaw of SNL mice were significantly decreased at 15, 30, 45, 60, 90 and 120 min post-injection compared with the corresponding SNL plus vehicle mice (Fig. 2A). The paw withdrawal latencies of the ipsilateral hindpaw in response to both heat and cold stimuli in SNL mice were markedly increased at 15, 30, 45, 60, 90, and 120 min post-injection compared to the corresponding SNL plus vehicle mice (Fig. 2B and 2C).

The effects of L524–0366 were dose-dependent (Fig. 2D-2F). L524–0366 at the dose of 10 μg produced significant reductions in paw withdrawal frequency to mechanical stimulation at 15, 30, 45, 60 and 90 min post-injection (Fig. 2D) and a marked increase in paw withdrawal latency to heat stimulation at 15 min post-injection (Fig. 2E) on the ipsilateral side of SNL mice compared with the SNL plus vehicle mice. L524–0366 at the dose of 10 μg had no effects on SNL-induced significant reductions in paw withdrawal latency to cold stimulation at any observation time points (Fig. 2F). There were no differences in paw withdrawal responses to mechanical, heat, and cold stimuli between the 5 μg L524–0366 plus SNL group and vehicle plus SNL groups (Fig. 2D-2F). L524–0366 at the dosage used did not change locomotor functions (Supplementary Table 2) or basal paw withdrawal responses mechanical, heat, and cold stimuli on the contralateral side of SNL mice or on both ipsilateral and contralateral sides of sham mice (Fig. 2A-2C; Supplementary Fig. 1A-1D).

Blocking the increased DRG Fn14 attenuates SNL-induced neuropathic pain

Intrathecal L524–0366 may lack the anatomical and pharmacological specificity. To further confirm the role of DRG Fn14 in neuropathic pain, we examined whether blocking the SNL-induced increase in DRG Fn14 through microinjection of AAV5 expressing Fn14 shRNA (AAV5-Fn14 shRNA) into the ipsilateral L4 DRG, affected SNL-induced pain hypersensitivity. The AAV5 harboring scrambled shRNA (AAV5-scramble shRNA) was used as the control. Consistent with the observation above, SNL led to significant increases in paw withdrawal frequency to mechanical stimulation and decreases in paw withdrawal latencies to heat and cold stimuli from days 3 to 14 post-SNL on the ipsilateral side of the AAV5-scramble shRNA-treated mice (Fig. 3A-3C). However, the SNL mice pre-

microinjected with AAV5-Fn14 shRNA displayed the attenuations in the increased paw withdrawal responses to mechanical stimulation and in the decreased paw withdrawal responses to heat and cold stimuli from days 3 to 14 post-SNL on the ipsilateral side as compared to the corresponding AAV5-scramble shRNA-treated SNL mice (Fig. 3A-3C). Neither AVV5-Fn14 shRNA nor AAV5-scramble shRNA altered locomotor functions (Supplementary Table 2) and basal paw withdrawal responses to mechanical, heat, and cold stimuli on the contralateral side of SNL mice and on the ipsilateral and contralateral sides of sham mice (Fig. 3A-3E).

After behavioral tests, we collected the ipsilateral L4 DRG on day 14 post-surgery and verified the expression of Fn14 in DRG. As expected, the level of Fn14 protein was increased by 3.2-fold in the ipsilateral L4 DRG of the AAV5-scramble shRNA-treated SNL mice as compared to that in the AAV5-scramble shRNA-treated sham mice (Fig. 3F). This increase was not seen in the SNL mice pre-microinjected with AAV5-Fn14 shRNA (Fig. 3F). The amount of Fn14 protein in the ipsilateral L4 DRG of the AAV5-Fn14 shRNA-treated SNL mice was reduced by 49% compared to the AAV5-scramble shRNA-treated SNL mice. No significant decrease in the amount of Fn14 protein was observed in the ipsilateral L4 DRG of the sham mice pre-microinjected with AAV5-Fn shRNA (Fig. 3F). The evidence revealed that AAV5-Fn14 shRNA could block the SNL-induced increase in Fn14 protein expression in the injured DRG.

Mimicking the SNL-induced increase in DRG Fn14 leads to pain hypersensitivity

We then determined whether mimicking the SNL-induced increase in DRG Fn14 expression through microinjection of AAV5 expressing full-length *Tnfrsf12a* mRNA (AAV5-Fn14) into unilateral L3/4 DRGs altered nociceptive thresholds in naïve mice. AAV5 expressing green fluorescent protein (AAV5-GFP) was used as the control. As expected, the level of Fn14 protein in the ipsilateral L3/4 DRGs of the AAV5-Fn-microinjected mice was increased by 1.5-fold compared to that in the AAV5-GFP-microinjected mice after behavioral tests on week 9 post-viral microinjection (Fig. 4A). Behaviorally. microinjection of AAV5-Fn14, but not AAV5-GFP, produced mechanical allodynia, thermal hyperalgesia, and cold allodynia as evidenced by the ipsilateral increases in paw withdrawal frequencies in response to mechanical stimuli (Fig. 4B) and by the ipsilateral decreases in paw withdrawal latencies in response to heat (Fig. 4C) and cold (Fig. 4D) stimuli. These pain hypersensitivities developed between 4–5weeks and persisted for at least 9 weeks (Fig. 4B-4D). Viral microinjection did not affect locomotor functions (Supplementary Table 2) or basal paw responses to mechanical, heat, and cold stimuli on the contralateral side (Fig. 4B-4D).

In addition to stimulation-evoked pain hypersensitivities, we also tested whether mimicking the SNL-induced increase in DRG Fn14 produced spontaneous ongoing nociceptive responses using a conditional place preference (CPP) paradigm on week 8 post-viral microinjection. The AAV5-Fn14-microinjected mice displayed an obvious preference for spending time in the lidocaine-paired chamber (Fig. 4E-4F), indicating stimulation-independent spontaneous nociceptive responses. As predicted, the AAV5-GFP-microinjected mice did not exhibit significant preference toward either the saline- or lidocaine-paired chamber (Fig. 4E-4F). Together, these findings indicate that mimicking the SNL-induced

increase in DRG Fn14 leads to both spontaneous and evoked pain hypersensitivities, typical symptoms of neuropathic pain in the clinic, in the absence of nerve injury. These pain hypersensitivities were further supported by the increases in expression of the biomarkers for cell activity in spinal cord dorsal horn. The levels of p-ERK1/2 (a marker for neuronal hyperactivation) and GFAP (a marker for astrocyte hyperactivation) significantly increased in the ipsilateral L3/4 dorsal horn of the AAV5 Fn14-microinjected mice as compared to that in the AAV5-GFP-microinjected mice on week 9 post-viral microinjection (Fig. 5A and 5B). No significant differences in the amounts of total ERK1/2 were seen in the ipsilateral L3/4 dorsal horn between two virial microinjected groups (Fig. 5A and 5B).

The increased Fn14 activates NF-κB pathway in the ipsilateral DRG after SNL

Given that nerve injury-induced DRG NF-κB pathway activation contributed to neuropathic pain and that NF-κB pathway was a potential downstream of Fn14 [10,34–36], we finally examined whether blocking the SNL-induced increase in DRG Fn14 participated in the activation of DRG NF-κB pathway under neuropathic pain conditions. The activation of NF-κB pathway was evidenced by the translocation of p65, a key member of NF-κB family, from cellular cytoplasm to nucleus [37–39]. The expression of p65 protein expression was markedly increased in the nucleus of the ipsilateral L4 DRG cells on day 14 after SNL in mice pre-microinjected with AAV5-scramble shRNA (Fig. 6A-6B), although the level of total p65 protein was not altered in the ipsilateral L4 DRG cells of the AAV5-scramble shRNA-microinjected mice on day 14 after SNL, when compared to the AAV5-scramble shRNA-microinjected sham mice (Fig. 6A and 6B). This increase was significantly hindered in the AAV5-Fn14 shRNA-microinjected mice (Fig. 6A and 6B). Microinjection of AAV5-Fn14-shRNA did not dramatically change basal expression of p65 protein in the nucleus of the ipsilateral L4 DRG cells of sham mice or basal expression of total p65 in the ipsilateral L4 DRG cells of sham or SNL mice (Fig. 6A and 6B). Single-cell reverse transcription polymerase chain reaction (RT-PCR) analysis revealed the co-expression of *Tnfrsf12a* (encoding Fn14 protein) and *Rela* (encoding p65 protein) in individual small, medium, and large DRG neurons (Fig. 6C-6E). These results revealed that Fn14 might activate the NF-κB pathway in the ipsilateral DRG after SNL.

Discussion

Peripheral nerve injury caused by SNL leads to mechanical allodynia, thermal hyperalgesia, and cold allodynia in mice, which mimics trauma/surgery-induced neuropathic pain in the clinic. In this study, we demonstrated that SNL led to an increase in Fn14 expression at both mRNA and protein levels in the ipsilateral DRG and that this increase contributed to neuropathic pain through an activation of the transcription factor NF-κB pathway in the DRG. Our findings suggest that Fn14 may be a potential target for the therapeutic treatment of peripheral neuropathic pain.

Fn14 is widely expressed in various tissues including heart, brain, kidney, colon, skeletal muscle. The level of Fn14 expression is rather low in most normal tissues and is rapidly up-regulated in response to tissue injury and inflammation under pathological conditions including rheumatoid arthritis, multiple sclerosis, inflammatory liver diseases, and

inflammatory bowel disease [12–16]. Fn14 plays an important role in the pathogenesis of nerve system diseases, such as neuropsychiatric disease, multiple sclerosis, and cerebral ischemia [18–20]. For example, Fn14 mRNA increases in ischemic brain at the early period after the onset of middle cerebral artery occlusion (MCAO) and inhibition of Fn14 early after MCAO was protective [20]. However, whether and how Fn14 contributes to neuropathic pain was not reported previously.

The *Tnfrsf12a* gene in the DRG can be activated at the transcriptional level in the response to peripheral nerve injury. A previous report revealed that *Tnfrsf12a* mRNA expression was increased 1 d after axotomy of sciatic nerve and persisted for at least 4–7 days postoperatively in the injured DRG, although basal *Tnfrsf12a* mRNA was barely detectable [18]. By *in situ* hybridization, this increase was demonstrated to occur at the injured DRG neurons [18]. Consistent with this observation, the present study further confirmed that the amounts of *Tnfrsf12a* mRNA and Fn14 protein were time-dependently and significantly elevated in the injured DRG, but not in intact DRG, after SNL or CCI. Due to current commercial unavailability of Fn14 antibody for immunostaining, the detailed subpopulation distribution of Fn14-positive neurons in the DRG post-SNL remains to be determined. Additionally, how peripheral nerve injury triggers the transcriptional activation of *Tnfrsf12a* gene under neuropathic pain conditions is still elusive. The potential possibilities, such as the changes in epigenetic modifications and increases in transcription factor expression and/or mRNA stability that may produce an elevation of *Tnfrsf12a* mRNA following peripheral nerve injury, could not be ruled out.

The contribution of the increased DRG Fn14 to neuropathic pain was demonstrated in this study not only by intrathecal administration of the specific Fn14 inhibitor L542–0366, but also by blocking the increased DRG Fn14 through microinjection of AAV5-Fn14 shRNA into the injured DRG. Unexpectedly, microinjection of AAV5-Fn14 shRNA did not significantly decrease the level of Fn14 expression in sham DRG. The reason for no effect of AAV5-Fn14 shRNA on basal Fn14 expression is unknown, but it may be related to lower basal level of DRG Fn14 expression. AAV5-Fn14 shRNA given at current volume and title likely cannot further lead to a significant reduction in DRG Fn14 at baseline.

The NF-KB pathway may mediate the role of the increased DRG Fn14 in neuropathic pain. It is well documented that NF-κB, a nuclear transcription factor, controls numerous genes encoding inflammatory cytokines and nociceptive mediators and plays a key role in neuropathic pain genesis [32,40,41]. Peripheral nerve injury activates NF-κB signaling in the DRG [42,3,43]. Intrathecal administration of pyrrolidine dithiocarbamate, an inhibitor of NF-κB, alleviates neuropathic pain and neuro-inflammation [41–44]. The present study revealed that blocking the increased DRG Fn14 expression attenuated SNL-induced nuclear translocation of NF-κB subunit p65 in the injured DRG. Given that *Tnfrsf12a* mRNA (encoding Fn14 protein) co-expresses with *Rela* mRNA (encoding p65 protein) in individual DRG neurons, Fn14 is very likely required for the activation of NF-κB signaling in the DRG neurons under neuropathic pain conditions. Whether the increased DRG Fn14 triggers other cellular signals following peripheral nerve injury is unknown, but DRG Fn14 contributes to neuropathic pain at least in part through the activation of the NF-κB pathway in the DRG neurons.

Conclusions

In conclusion, our present study reveals that pharmacological inhibition or genetic knockdown of DRG increased Fn14 displays significant effects on peripheral nerve injury-induced pain hypersensitivities, without altering basal or acute nociceptive responses and locomotor functions. These findings suggest that Fn14 may be a potential target for the management of neuropathic pain. However, it is worth noting that Fn14 is expressed in other tissues besides DRG and may target other cellular signaling pathways in addition to NF-κB. Therefore, careful attention should be paid to potential adverse effects caused by Fn14 inhibitors.

Supplementary Material

Refer to Web version on PubMed Central for supplementary material.

Acknowledgments

Funding information

This work was supported by the grants (NS094664, NS094224, and DA033390) from the National Institutes of Health (Bethesda, Maryland, USA).

REFERENCES

1. DiBonaventura MD, Sadosky A, Concialdi K, Hopps M, Kudel I, Parsons B, Cappelleri JC, Hlavacek P, Alexander AH, Stacey BR, Markman JD, Farrar JT (2017) The prevalence of probable neuropathic pain in the US: results from a multimodal general-population health survey. Journal of pain research 10:2525–2538. doi:10.2147/JPR.S127014 [PubMed: 29138590]
2. van Hecke O, Austin SK, Khan RA, Smith BH, Torrance N (2014) Neuropathic pain in the general population: a systematic review of epidemiological studies. Pain 155 (4):654–662. doi:10.1016/j.pain.2013.11.013 [PubMed: 24291734]
3. Mitka M (2003) "Virtual textbook" on pain developed: effort seeks to remedy gap in medical education. Jama 290 (18):2395. doi:10.1001/jama.290.18.2395 [PubMed: 14612463]
4. Vorobeychik Y, Gordin V, Mao J, Chen L (2011) Combination therapy for neuropathic pain: a review of current evidence. CNS drugs 25 (12):1023–1034. doi:10.2165/11596280-000000000-00000 [PubMed: 22133325]
5. Dworkin RH, O'Connor AB, Kent J, Mackey SC, Raja SN, Stacey BR, Levy RM, Backonja M, Baron R, Harke H, Loeser JD, Treede RD, Turk DC, Wells CD (2013) Interventional management of neuropathic pain: NeuPSIG recommendations. Pain 154 (11):2249–2261. doi:10.1016/j.pain.2013.06.004 [PubMed: 23748119]
6. Yang DZ, Sin B, Beckhusen J, Xia D, Khaimova R, Iliev I (2018) Opioid-Induced Hyperalgesia in the Nonsurgical Setting: A Systematic Review. American journal of therapeutics doi:10.1097/MJT.0000000000000734
7. Raffa RB, Pergolizzi JV Jr. (2013) Opioid-induced hyperalgesia: is it clinically relevant for the treatment of pain patients? Pain management nursing : official journal of the American Society of Pain Management Nurses 14 (3):e67–83. doi:10.1016/j.pmn.2011.04.002 [PubMed: 23972873]
8. Bekhit MH (2010) Opioid-induced hyperalgesia and tolerance. American journal of therapeutics 17 (5):498–510. doi:10.1097/MJT.0b013e3181ed83a0 [PubMed: 20844348]
9. Meyer R, Patel AM, Rattana SK, Quock TP, Mody SH (2014) Prescription opioid abuse: a literature review of the clinical and economic burden in the United States. Population health management 17 (6):372–387. doi:10.1089/pop.2013.0098 [PubMed: 25075734]
10. Polavarapu R, Gongora MC, Winkles JA, Yepes M (2005) Tumor necrosis factor-like weak inducer of apoptosis increases the permeability of the neurovascular unit through nuclear factor-kappa B

pathway activation. The Journal of neuroscience : the official journal of the Society for Neuroscience 25 (44):10094–10100. doi:10.1523/JNEUROSCI.3382-05.2005 [PubMed: 16267216]

11. Qi X, Qin L, Du R, Chen Y, Lei M, Deng M, Wang J (2017) Lipopolysaccharide Upregulated Intestinal Epithelial Cell Expression of Fn14 and Activation of Fn14 Signaling Amplify Intestinal TLR4-Mediated Inflammation. Frontiers in cellular and infection microbiology 7:315. doi: 10.3389/fcimb.2017.00315 [PubMed: 28744451]
12. Liu Y, Xu M, Min X, Wu K, Zhang T, Li K, Xiao S, Xia Y (2017) TWEAK/Fn14 Activation Participates in Ro52-Mediated Photosensitization in Cutaneous Lupus Erythematosus. Frontiers in immunology 8:651. doi:10.3389/fimmu.2017.00651 [PubMed: 28620393]
13. Xia Y, Campbell SR, Broder A, Herlitz L, Abadi M, Wu P, Michaelson JS, Burkly LC, Putterman C (2012) Inhibition of the TWEAK/Fn14 pathway attenuates renal disease in nephrotoxic serum nephritis. Clin Immunol 145 (2):108–121. doi:10.1016/j.clim.2012.08.008 [PubMed: 22982296]
14. Zou Y, Bao S, Wang F, Guo L, Zhu J, Wang J, Deng X, Li J (2018) FN14 Blockade on Pulmonary Microvascular Endothelial Cells Improves the Outcome of Sepsis-Induced Acute Lung Injury. Shock 49 (2):213–220. doi:10.1097/SHK.0000000000000915 [PubMed: 28562476]
15. Sato S, Ogura Y, Kumar A (2014) TWEAK/Fn14 Signaling Axis Mediates Skeletal Muscle Atrophy and Metabolic Dysfunction. Frontiers in immunology 5:18. doi:10.3389/fimmu. 2014.00018 [PubMed: 24478779]
16. Mittal A, Bhatnagar S, Kumar A, Lach-Trifilieff E, Wauters S, Li H, Makonchuk DY, Glass DJ (2010) The TWEAK-Fn14 system is a critical regulator of denervation-induced skeletal muscle atrophy in mice. The Journal of cell biology 188 (6):833–849. doi:10.1083/jcb.200909117 [PubMed: 20308426]
17. Wilhelm A, Shepherd EL, Amatucci A, Munir M, Reynolds G, Humphreys E, Resheq Y, Adams DH, Hubscher S, Burkly LC, Weston CJ, Afford SC (2016) Interaction of TWEAK with Fn14 leads to the progression of fibrotic liver disease by directly modulating hepatic stellate cell proliferation. The Journal of pathology 239 (1):109–121. doi:10.1002/path.4707 [PubMed: 26924336]
18. Tanabe K, Bonilla I, Winkles JA, Strittmatter SM (2003) Fibroblast growth factor-inducible-14 is induced in axotomized neurons and promotes neurite outgrowth. The Journal of neuroscience : the official journal of the Society for Neuroscience 23 (29):9675–9686 [PubMed: 14573547]
19. Yepes M (2007) TWEAK and the central nervous system. Molecular neurobiology 35 (3):255–265 [PubMed: 17917114]
20. Yepes M (2007) Tweak and FN14 in central nervous system health and disease. Frontiers in bioscience : a journal and virtual library 12:2772–2781 [PubMed: 17485258]
21. Desplat-Jego S, Creidy R, Varriale S, Allaire N, Luo Y, Bernard D, Hahm K, Burkly L, Boucraut J (2005) Anti-TWEAK monoclonal antibodies reduce immune cell infiltration in the central nervous system and severity of experimental autoimmune encephalomyelitis. Clin Immunol 117 (1):15–23. doi:10.1016/j.clim.2005.06.005 [PubMed: 16027043]
22. Wen J, Chen CH, Stock A, Doerner J, Gulinello M, Putterman C (2016) Intracerebroventricular administration of TNF-like weak inducer of apoptosis induces depression-like behavior and cognitive dysfunction in non-autoimmune mice. Brain, behavior, and immunity 54:27–37. doi: 10.1016/j.bbi.2015.12.017
23. Frauenknecht K, Bargiotas P, Bauer H, von Landenberg P, Schwaninger M, Sommer C (2010) Neuroprotective effect of Fn14 deficiency is associated with induction of the granulocyte-colony stimulating factor (G-CSF) pathway in experimental stroke and enhanced by a pathogenic human antiphospholipid antibody. Journal of neuroimmunology 227 (1–2):1–9. doi:10.1016/j.jneuroim. 2010.05.043 [PubMed: 20557950]
24. Pelekanou V, Notas G, Kampa M, Tsentelierou E, Stathopoulos EN, Tsapis A, Castanas E (2013) BAFF, APRIL, TWEAK, BCMA, TACI and Fn14 proteins are related to human glioma tumor grade: immunohistochemistry and public microarray data meta-analysis. PloS one 8 (12):e83250. doi:10.1371/journal.pone.0083250 [PubMed: 24376672]
25. Rigaud M, Gemes G, Barabas ME, Chernoff DI, Abram SE, Stucky CL, Hogan QH (2008) Species and strain differences in rodent sciatic nerve anatomy: implications for studies of neuropathic pain. Pain 136 (1–2):188–201. doi:10.1016/j.pain.2008.01.016 [PubMed: 18316160]

26. Li Z, Gu X, Sun L, Wu S, Liang L, Cao J, Lutz BM, Bekker A, Zhang W, Tao YX (2015) Dorsal root ganglion myeloid zinc finger protein 1 contributes to neuropathic pain after peripheral nerve trauma. Pain 156 (4):711–721. doi:10.1097/j.pain.0000000000000103 [PubMed: 25630025]
27. Zhao X, Tang Z, Zhang H, Atianjoh FE, Zhao JY, Liang L, Wang W, Guan X, Kao SC, Tiwari V, Gao YJ, Hoffman PN, Cui H, Li M, Dong X, Tao YX (2013) A long noncoding RNA contributes to neuropathic pain by silencing Kcna2 in primary afferent neurons. Nature neuroscience 16 (8): 1024–1031. doi:10.1038/nn.3438 [PubMed: 23792947]
28. Liaw WJ, Zhu XG, Yaster M, Johns RA, Gauda EB, Tao YX (2008) Distinct expression of synaptic NR2A and NR2B in the central nervous system and impaired morphine tolerance and physical dependence in mice deficient in postsynaptic density-93 protein. Molecular pain 4:45. doi: 10.1186/1744-8069-4-45 [PubMed: 18851757]
29. He Y, Tian X, Hu X, Porreca F, Wang ZJ (2012) Negative reinforcement reveals non-evoked ongoing pain in mice with tissue or nerve injury. The journal of pain : official journal of the American Pain Society 13 (6):598–607. doi:10.1016/j.jpain.2012.03.011 [PubMed: 22609247]
30. Tao YX, Rumbaugh G, Wang GD, Petralia RS, Zhao C, Kauer FW, Tao F, Zhuo M, Wenthold RJ, Raja SN, Huganir RL, Bredt DS, Johns RA (2003) Impaired NMDA receptor-mediated postsynaptic function and blunted NMDA receptor-dependent persistent pain in mice lacking postsynaptic density-93 protein. The Journal of neuroscience : the official journal of the Society for Neuroscience 23 (17):6703–6712 [PubMed: 12890763]
31. Wu S, Marie Lutz B, Miao X, Liang L, Mo K, Chang YJ, Du P, Soteropoulos P, Tian B, Kaufman AG, Bekker A, Hu Y, Tao YX (2016) Dorsal root ganglion transcriptome analysis following peripheral nerve injury in mice. Molecular pain 12. doi:10.1177/1744806916629048
32. Guo D, Hu X, Zhang H, Lu C, Cui G, Luo X (2018) Orientin and neuropathic pain in rats with spinal nerve ligation. International immunopharmacology 58:72–79. doi:10.1016/j.intimp. 2018.03.013 [PubMed: 29558662]
33. Liang L, Zhao JY, Gu X, Wu S, Mo K, Xiong M, Marie Lutz B, Bekker A, Tao YX (2016) G9a inhibits CREB-triggered expression of mu opioid receptor in primary sensory neurons following peripheral nerve injury. Molecular pain 12. doi:10.1177/1744806916682242
34. Yepes M, Brown SA, Moore EG, Smith EP, Lawrence DA, Winkles JA (2005) A soluble Fn14-Fc decoy receptor reduces infarct volume in a murine model of cerebral ischemia. The American journal of pathology 166 (2):511–520. doi:10.1016/S0002-9440(10)62273-0 [PubMed: 15681834]
35. Hosokawa Y, Hosokawa I, Shindo S, Ozaki K, Nakae H, Matsuo T (2012) Tumor necrosis factor-like weak inducer of apoptosis increases CC chemokine ligand 20 production in interleukin 1beta-stimulated human gingival fibroblasts. Human immunology 73 (5):470–473. doi:10.1016/ j.humimm.2012.02.021 [PubMed: 22425737]
36. Echeverry R, Wu F, Haile WB, Wu J, Yepes M (2012) The cytokine tumor necrosis factor-like weak inducer of apoptosis and its receptor fibroblast growth factor-inducible 14 have a neuroprotective effect in the central nervous system. Journal of neuroinflammation 9:45. doi: 10.1186/1742-2094-9-45 [PubMed: 22394384]
37. Bao Q, Li C, Xu C, Zhang R, Zhao K, Duan Z (2018) Porcine enterocyte protein Btnl5 negatively regulates NF-kappa B pathway by interfering p65 nuclear translocation. Gene 646:47–55. doi: 10.1016/j.gene.2017.11.070 [PubMed: 29197592]
38. Zhang YC, Huo FC, Wei LL, Gong CC, Pan YJ, Mou J, Pei DS (2017) PAK5-mediated phosphorylation and nuclear translocation of NF-kappaB-p65 promotes breast cancer cell proliferation in vitro and in vivo. Journal of experimental & clinical cancer research : CR 36 (1): 146. doi:10.1186/s13046-017-0610-5 [PubMed: 29041983]
39. Tomita H, Tabata K, Takahashi M, Nishiyama F, Sugano E (2016) Light induces translocation of NF-kappaB p65 to the mitochondria and suppresses expression of cytochrome c oxidase subunit III (COX III) in the rat retina. Biochemical and biophysical research communications 473 (4): 1013–1018. doi:10.1016/j.bbrc.2016.04.008 [PubMed: 27055596]
40. Chen Y, Chen X, Yu J, Xu X, Wei X, Gu X, Liu C, Zhang D, Xu Z (2016) JAB1 is Involved in Neuropathic Pain by Regulating JNK and NF-kappaB Activation After Chronic Constriction Injury. Neurochemical research 41 (5):1119–1129. doi:10.1007/s11064-015-1802-z [PubMed: 26700435]

41. Xu T, Li D, Zhou X, Ouyang HD, Zhou LJ, Zhou H, Zhang HM, Wei XH, Liu G, Liu XG (2017) Oral Application of Magnesium-L-Threonate Attenuates Vincristine-induced Allodynia and Hyperalgesia by Normalization of Tumor Necrosis Factor-alpha/Nuclear Factor-kappaB Signaling. Anesthesiology 126 (6):1151–1168. doi:10.1097/ALN.0000000000001601 [PubMed: 28306698]

42. Yu HM, Wang Q, Sun WB (2017) Silencing of FKBP51 alleviates the mechanical pain threshold, inhibits DRG inflammatory factors and pain mediators through the NF-kappaB signaling pathway. Gene 627:169–175. doi:10.1016/j.gene.2017.06.029 [PubMed: 28629826]

43. Zhang HH, Hu J, Zhou YL, Hu S, Wang YM, Chen W, Xiao Y, Huang LY, Jiang X, Xu GY (2013) Promoted interaction of nuclear factor-kappaB with demethylated cystathionine-beta-synthetase gene contributes to gastric hypersensitivity in diabetic rats. The Journal of neuroscience : the official journal of the Society for Neuroscience 33 (21):9028–9038. doi:10.1523/JNEUROSCI.1068-13.2013 [PubMed: 23699514]

44. Zhang HH, Hu J, Zhou YL, Qin X, Song ZY, Yang PP, Hu S, Jiang X, Xu GY (2015) Promoted Interaction of Nuclear Factor-kappaB With Demethylated Purinergic P2X3 Receptor Gene Contributes to Neuropathic Pain in Rats With Diabetes. Diabetes 64 (12):4272–4284. doi:10.2337/db15-0138 [PubMed: 26130762]

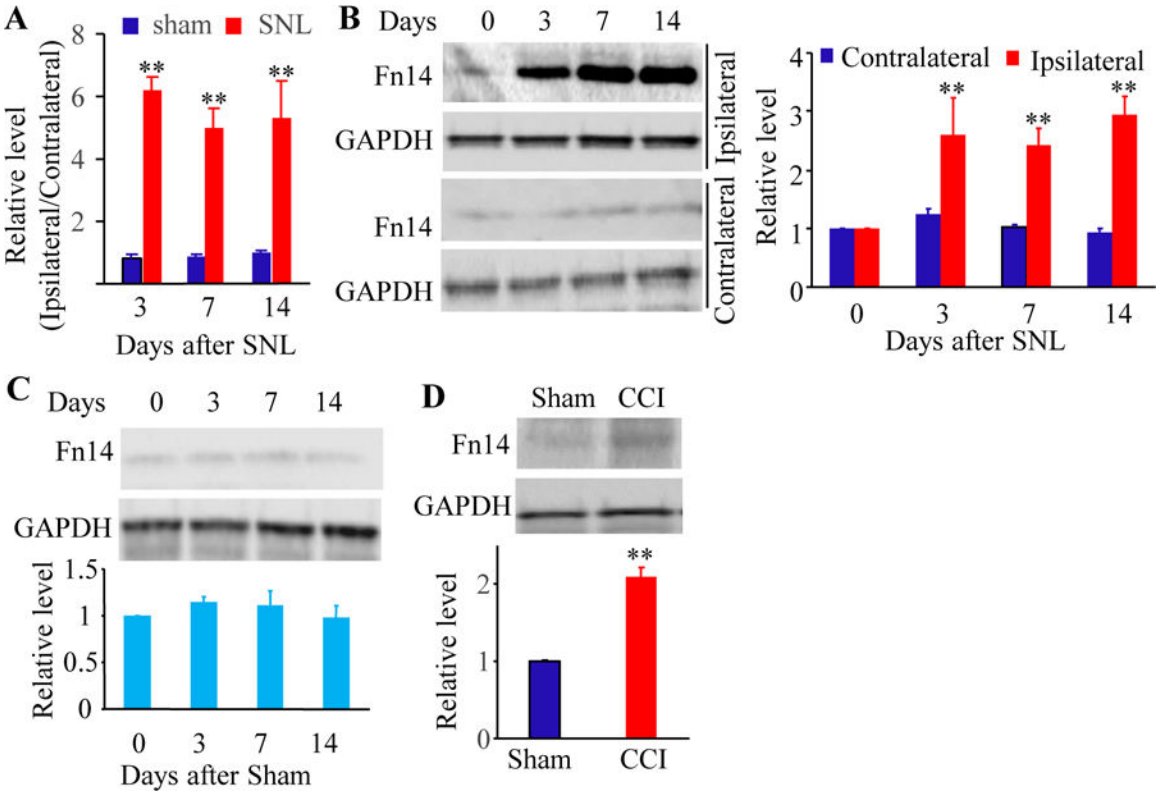

Fig. 1.

Peripheral nerve injury-induced increases in *Tnfrsf12a* mRNA and Fn14 protein in the ipsilateral L4 DRG. (A) *Tnfrsf12a* mRNA expression in the ipsilateral and contralateral L4 DRG after SNL or sham surgery. Unilateral L4 DRGs from four mice were pooled together. n = 3 biological replicates (12 mice) per time point. Two-way analysis of variance (ANOVA) followed by Tukey post hoc test. $^{**}P < 0.01$ *vs* the corresponding sham group. (B) Fn14 protein expression in the ipsilateral and contralateral L4 DRG after SNL. Representative Western blots (left) and a summary of densitometric analysis (right) are shown. n = 3 biological replicates (12 mice) per time point. Two-way analysis of variance (ANOVA) followed by Tukey post hoc test. $^{**}P < 0.01$ *vs* the corresponding contralateral side. (C) Fn14 protein expression in the ipsilateral L4 DRG after sham surgery. n = 3 biological replicates (12 mice) per time point. Two-way analysis of variance (ANOVA) followed by Tukey post hoc test. (D) Fn14 protein expression in the ipsilateral L3 DRG after SNL. Representative Western blots and a summary of densitometric analysis are shown. n = 3 biological replicates (12 mice) per group. (E) Fn14 protein expression in the ipsilateral L3/L4 DRGs on day 7 after CCI or sham surgery. Representative Western blots and a summary of densitometric analysis are shown. n = 3 biological replicates (6 mice) per group. Two-tailed, independent Student's *t* test. $^{**}P < 0.01$ *vs* the sham group.

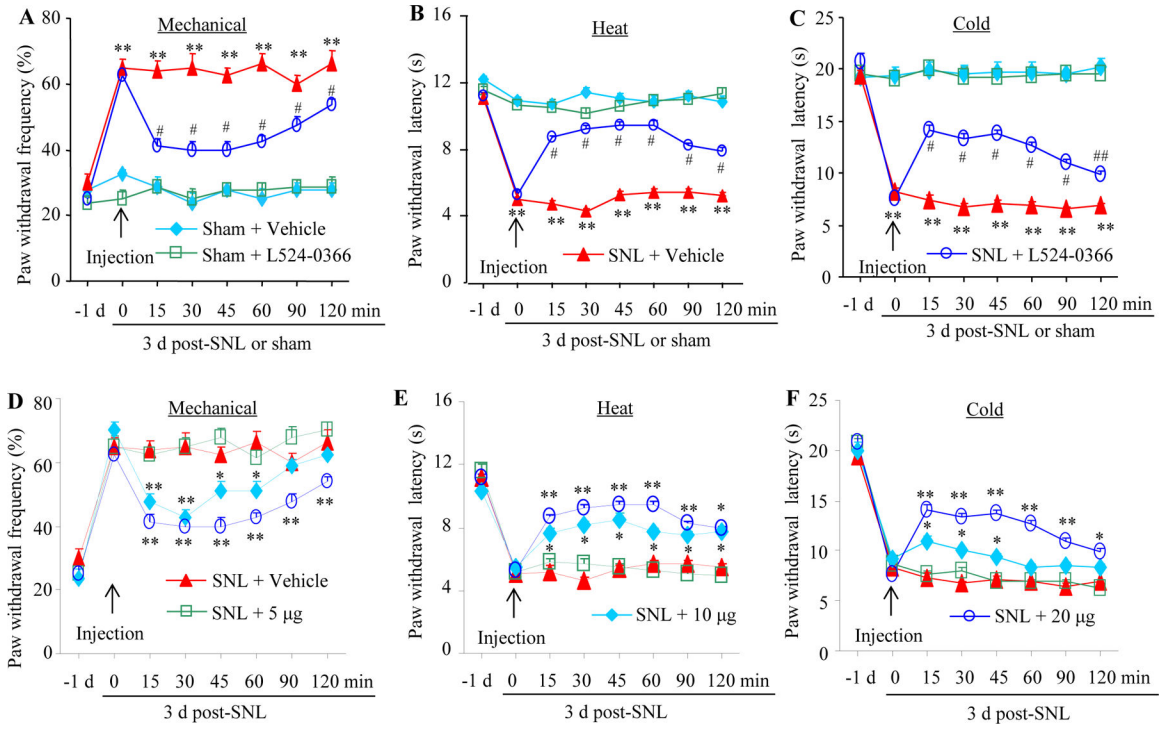

Fig. 2.

Effect of intrathecal Fn14 inhibitor L524–0366 on SNL-induced neuropathic pain on the ipsilateral side. (A to C) Effect of intrathecal vehicle or 20 μg L524–0366 on paw withdrawal frequencies to mechanical stimulation (A), paw withdrawal latencies to heat (B) and cold (C) stimuli on 3 day post-SNL or sham surgery. n = 8 mice/group. Two-way analysis of variance (ANOVA) followed by Tukey post hoc test. $*P < 0.05$ or $**P < 0.01$ *vs* the sham plus vehicle group at the corresponding time point. $\#P < 0.05$ or $\#\#P < 0.01$ *vs* the SNL plus vehicle group at the corresponding time point. (D to F) Dose-dependent effect of intrathecal L524–0366 or vehicle on paw withdrawal frequency to mechanical stimuli (D) and paw withdrawal latencies to heat (E) and cold (F) stimuli on day 3 post-SNL or sham surgery. n = 8 mice/group. Two-way analysis of variance (ANOVA) followed by Tukey post hoc test. $*P < 0.05$ or $**P < 0.01$ *vs* the SNL plus vehicle group at the corresponding time point.

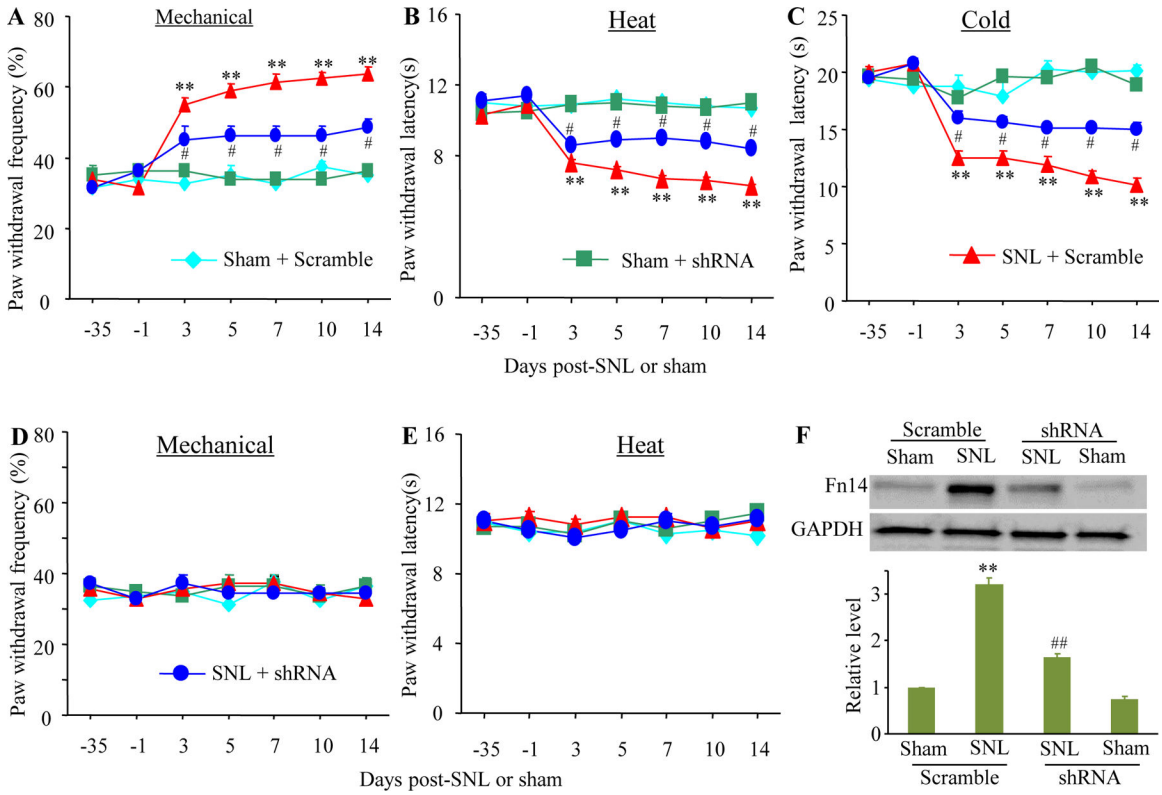

Fig. 3.

Effect of DRG microinjection of AAV5-Fn14 shRNA on SNL-induced neuropathic pain. (A to E) Effect of DRG microinjection of AAV5-Fn14 shRNA or AAV5-scramble shRNA on paw withdrawal frequencies to mechanical stimulation (A and D), paw withdrawal latencies to heat (B and E) and cold (C) stimuli on the ipsilateral (A to C) and contralateral (D and E) sides at different time points after SNL or sham surgery. n = 12 mice/group. Two-way analysis of variance (ANOVA) followed by Tukey post hoc test. $^{**}P < 0.01$ *vs* the sham plus scramble group at the corresponding day. $\#P < 0.05$ *vs* the SNL plus scramble group at the corresponding day. (F) Fn14 protein expression in the ipsilateral L4 DRG of the AAV5-Fn14 shRNA-injected or AAV5-scramble shRNA-injected mice on day 14 after SNL or sham surgery. Unilateral L4 DRGs from four mice were pooled together. n = 3 biological replicates (12 mice) per group. One-way analysis of variance (ANOVA) followed by Tukey post hoc test. $^{**}P < 0.01$ *vs* the sham plus scramble group. $\#\#P < 0.01$ *vs* the SNL plus scramble group.

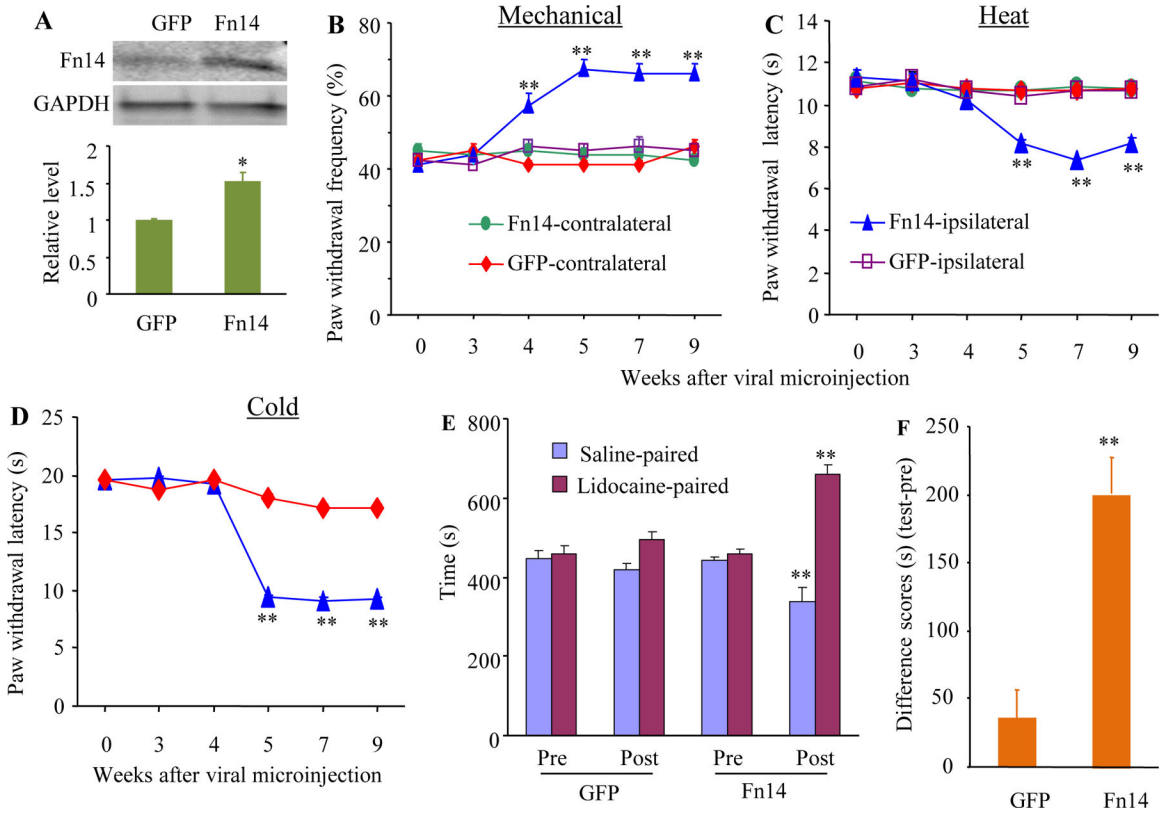

Fig. 4.

Effect of DRG Fn14 overexpression on nociceptive thresholds in naïve mice. (A) Fn14 protein expression in the injected L3/4 DRGs 9 weeks after microinjection of AAV5-Fn14 or control AAV5-GFP. n = 5 biological replicates (10 mice)/group. Two-tailed, independent Student's *t* test, $*P < 0.05$ *vs* the AAV5-GFP group. (B to D) Effect of microinjection of AAV5-Fn14 or control AAV5-GFP into the unilateral L3/4 DRGs on paw withdrawal frequencies to mechanical stimulation (B) and paw withdrawal latencies to heat (C) and cold (D) stimuli (D) on the ipsilateral and contralateral sides at different weeks after viral microinjection. n = 10 mice/group. Two-way analysis of variance (ANOVA) followed by Tukey post hoc test. $**P < 0.01$ *vs* the control AAV5-GFP group on the ipsilateral side at the corresponding time points. (E and F) Effect of microinjection of AAV5-Fn14 or control AAV5-GFP into the unilateral L3/4 DRGs on spontaneous ongoing pain as assessed by CPP paradigm. Pre: preconditioning. Post: Postconditioning. n =10 mice/group. $**P < 0.01$ *vs* the corresponding preconditioning by two-way analysis of variance (ANOVA) followed by Tukey post hoc test (E) or the AAV5-GFP group by two-tailed, independent Student's *t* test (F).

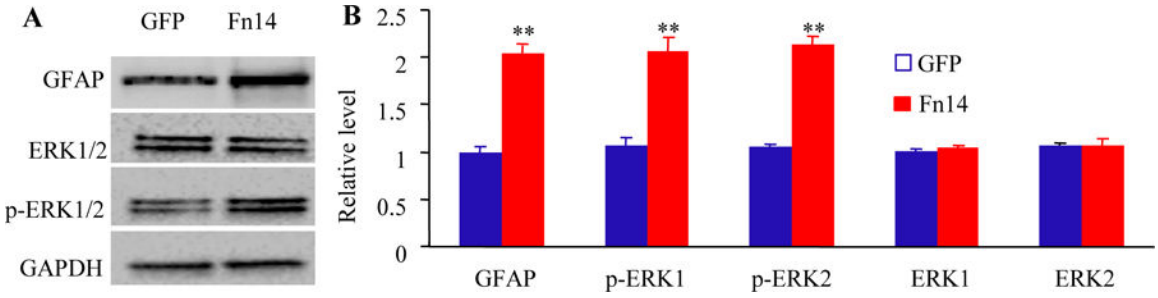

Fig. 5.

Effect of microinjection of AAV5-Fn14 or control AAV5-GFP into the unilateral L3/4 DRGs on the expression of the phosphorylation of ERK 1/2 (p-ERK1/2) and GFAP in the ipsilateral L3/4 dorsal horn 9 weeks after viral microinjection. (A-B) Representative Western blots (A) and a summary of densitometric analysis (B) are shown. n = 5 biological replicates (10 mice) per group. $^{**}P < 0.01$ *vs* the AAV5-GFP group by two-tailed, independent Student's *t* test.

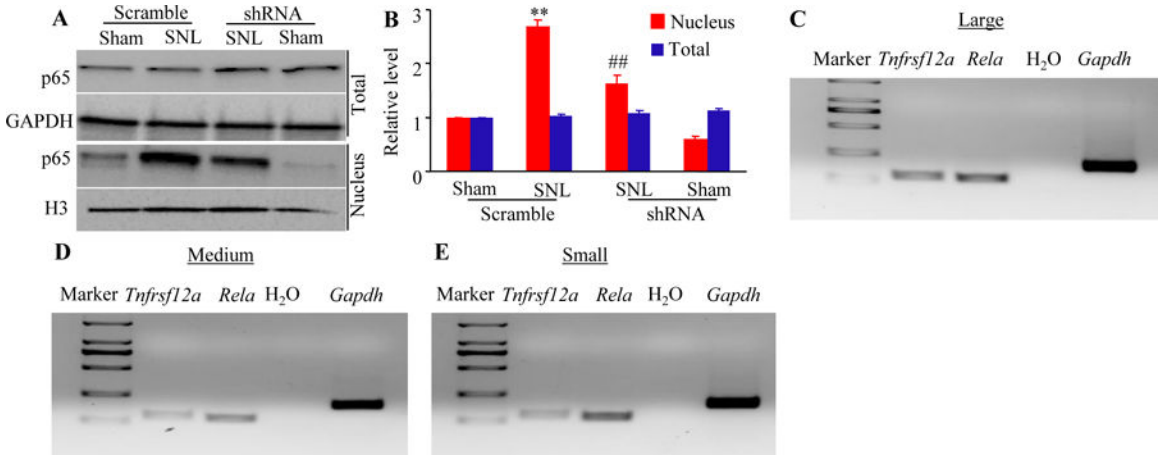

Fig. 6.

Fn14-triggered activation of the NF-κB pathway in the ipsilateral L4 DRG after SNL. (A-B) Expression of p65 protein in total and nuclear fractions from the injected L4 DRG of the mice pre-microinjected with AAV5-Fn14 shRNA or AAV5-scramble shRNA 14 days after SNL or sham surgery. Representative Western blots (A) and a summary of densitometric analysis (B) are shown. n = 3 biological replicates (12 mice) per group. One-way analysis of variance (ANOVA) followed by Tukey post hoc test. $^{**}P < 0.01$ *vs* the corresponding sham plus scramble group. $^{\#\#}P < 0.01$ *vs* the corresponding SNL plus scramble group. (C to E) Co-expression of *Tnfrsf12a* mRNA with *Rela* mRNA in large (C), medium (D), and small (E) DRG neurons. *Gapdh* mRNA was used as a positive control. n = 3 biological replicates.